

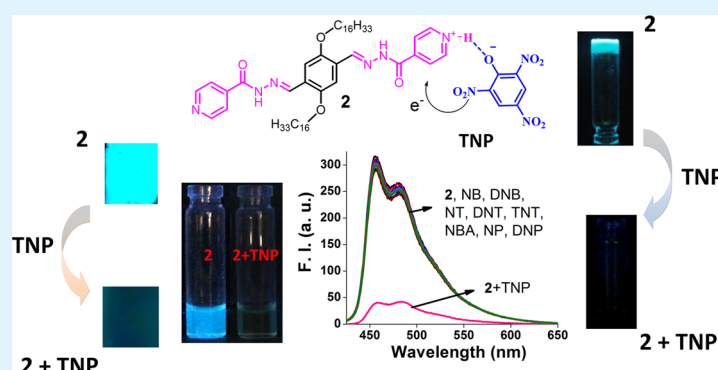
Selective and Efficient Detection of Nitro-Aromatic Explosives in Multiple Media including Water, Micelles, Organogel, and Solid Support

Nilanjan Dey,[†] Suman K. Samanta,[†] and Santanu Bhattacharya^{*,†,‡}

[†]Department of Organic Chemistry, Indian Institute of Science, Bangalore 560012, India

[‡]Jawaharlal Nehru Centre for Advanced Scientific Research, Bangalore 560064, India

Supporting Information



ABSTRACT: Selective detection of nitro-aromatic compounds (NACs) at nanomolar concentration is achieved for the first time in multiple media including water, micelles or in organogels as well as using test strips. Mechanism of interaction of NACs with highly fluorescent *p*-phenylenevinylene-based molecules has been described as the electron transfer phenomenon from the electron-rich chromophoric probe to the electron deficient NACs. The selectivity in sensing is guided by the pK_a of the probes as well as the NACs under consideration. TNP-induced selective gel-to-sol transition in THF medium is also observed through the reorganization of molecular self-assembly and the portable test strips are made successfully for rapid on-site detection purpose.

KEYWORDS: nitro-aromatic explosives, micellar medium, organogel, test strips, nanomolar detection

INTRODUCTION

Design of new probes for ultrasensitive and low cost detection of explosives are essential for applications in homeland security techniques, criminal and forensic sciences.¹ Recent rise in terrorist activity imposes necessity of rapid detection of explosives, e.g., TNT (2,4,6-trinitrotoluene), DNT (2,4-dinitrotoluene), and TNP (2,4,6-trinitrophenol, picric acid), as they are often the main components of most of the landmines.² Although a number of techniques (spectroscopic, electrochemical)^{3–5} and systems (nanoparticles,^{6–9} polymers^{10–15}) are known for the detection and quantification of these chemicals, small organic molecule-based probes for explosive detection has attracted particular attention toward this end.^{16–19} Recently, Zang et al.^{20,21} and Liu et al.²² have reported efficient vapor phase detection of nitro-aromatics (NACs) such as TNT, DNT, CH_3NO_2 , and DNP using fluorescent nanofibers prepared from small molecules based on either carbazole, or anthracene or porphyrin backbones. The electron deficiency of the NACs make them prone to interact with the electron-rich organic fluorescent molecules.²³ Although TNP is a superior explosive than TNT, only a few reports toward the detection of TNP have appeared compared

to that of TNT.^{24–27} Apart from its highly explosive nature, TNP also causes severe irritation, skin allergy, dizziness, nausea, damage of liver, and kidney.^{28,29} Water contamination of TNP may cause severe epidemic.^{30,31} In 2011, Wang et al. first developed a selective sensor for TNP based on isonicotinyldiazide in DMF medium.³² At the same time, some ICT-based probes for TNP detection were reported independently by Kumar et al.³³ and Pang et al.³⁴ Recently, imidazolium-based cationic probes or asymmetric triazine-based probes also appeared in the literature for picric acid sensing purpose.^{35–38} But in all these reports, sensing was mostly achieved in either organic media or in organic–water mixture media. In some cases, significant interference was also observed from other nitro aromatics. These limit the practical use of such sensors for the detection of TNP contamination in natural water sources, which is also a lethal threat for our ecosystem.

As a continuation of our efforts in developing small molecular sensors,^{39–41} we report herein new *p*-phenyl-

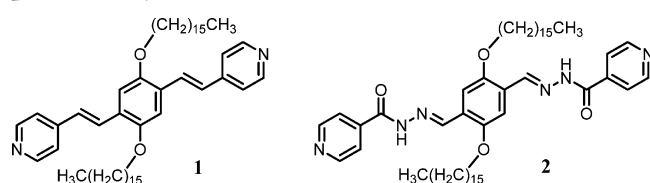
Received: April 30, 2013

Accepted: June 20, 2013

Published: June 20, 2013

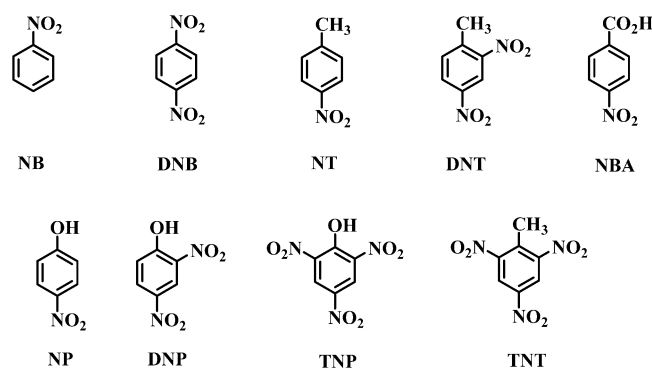
enevinylene based probes **1** and **2** (Chart 1) for the nanomolar detection of TNP in water. To the best of our knowledge, this

Chart 1. Structures of the molecular probes used in the present study



is the first report where an inexpensive micellar medium has been exploited for the detection of explosives in complete water (organic solvent <1%). At the same time, an instant 'naked eye' response of TNP detection using test strips could be established demonstrating it as an effective portable device for an on-site detection of such explosives. On the other hand, the effect of interaction of NACs (Chart 2) with each probe on

Chart 2. Structures of the Nitro Aromatics (NACs) Used in the Present Study



its supramolecular organization has been also addressed. This opens up another way of detection of NACs as in this case an addition of TNP causes selective transformation of gel-to-sol through the breakdown of the self-assembly of the probes in this particular instance.

EXPERIMENTAL SECTION

Materials and Instrumentations. All reagents, starting materials, and silica gel for TLC and column chromatography were obtained from the best known commercial sources and were used without further purification. Solvents were distilled and dried prior to use. FT-IR spectra were recorded on a Perkin-Elmer FT-IR Spectrum BX system and were reported in wave numbers (cm^{-1}). ^1H NMR and ^{13}C NMR spectra were recorded with a Bruker Advance DRX 400 spectrometer operating at 400 and 100 MHz for ^1H and ^{13}C NMR spectroscopy, respectively. Chemical shifts were reported in ppm downfield from the internal standard, tetramethylsilane (TMS). Mass spectra were recorded on Micromass Q-TOF Micro TM spectrometer.

Sampling Procedure of Sensing. Sensing of the NACs in pure water was carried out by adding 10 μL THF solution of either **1** or **2** from a stock (1×10^{-3} M) in pure water to make the final volume of 1 mL ($[\mathbf{1}] = [\mathbf{2}] = 1 \times 10^{-5}$ M) followed by addition of THF solution of the NACs (5 equiv. for **1** and 2 equiv. for **2**). In case of sensing in the micellar medium, 10 μL of the THF stock solution (1×10^{-3} M) of either **1** or **2** was added into the Brij-58 (1 mM), SDS (8 mM) or CTAB (1 mM) micellar solution to make the final volume of 1 mL. This was followed by addition of an aliquot of THF solution of the NACs (5 equiv. for **1** and 2 equiv. for **2**). Similar procedure has been

followed for the sensing in buffered media of different pH ($\text{HCO}_2\text{Na}/\text{HCl}$ buffer for pH 2, Tris/HCl for pH 7 and $\text{Na}_2\text{B}_4\text{O}_7 \cdot 10\text{H}_2\text{O}/\text{NaOH}$ for pH 12). The final concentration of THF in the solution did not exceed 1%. For sensing in the organic medium, 2 equiv. of NACs were directly added into the THF solution of **2** (1×10^{-5} M). The sensing in the gel medium was performed by adding solid NACs into the preformed THF gel of **2** (12 mg/mL, 14 mM) followed by gentle shaking to observe the abolition of the gel in situ.

UV-Vis and Fluorescence Spectroscopy. The UV-vis and fluorescence spectroscopy were recorded on a Shimadzu model 2100 spectrometer and Cary Eclipse spectrofluorimeter respectively. The slit-width for the fluorescence experiment was kept at 5 nm (excitation) and 5 nm (emission) and the excitation wavelength was set at 400 nm for **1**, and 390 nm for **2**.

Scanning Electron Microscopy. Solution of **2** (concentration 100 μM) alone and in presence of different NACs (2 equiv.) were drop cast over double-sided tapes attached onto the brass stubs and air-dried for 48 h. The samples were then coated with gold vapor and analyzed on a Quanta 200 SEM operated at 15 kV.

Gelation Studies and Determination of Minimum Gelator Concentration (MGC). Previously weighed amount of **2** in THF was taken in a sealed glass vial and heated till the solid completely dissolved to afford a transparent solution. The clear solution was left to cool under ambient condition at 25 $^\circ\text{C}$ without any external perturbation. Observations with regard to gelation were recorded from time to time. Each experiment was performed in duplicate. The state of the materials was checked by conventional "stable-to-inversion of a test tube" method. If the gel was formed, it was evaluated quantitatively by determining the minimum gelator concentration (MGC) which is the minimum amount of gelator required to immobilize 1 mL of a particular solvent. Gelation in presence of TNP was checked after heating and consequent cooling cycle.

^1H NMR Titration Studies. ^1H NMR titration with compound **1** and **2** were performed upon dissolving **1** (8 mM) in CDCl_3 and **2** (8 mM) in $\text{CDCl}_3/\text{CD}_3\text{OD}$ (5:1 v/v). To that TNP was added (0 to 1.5 equiv.) and the spectra were recorded using identical parameters.

Fluorescence Decay Experiment. Fluorescence lifetime values were measured by using a time-correlated single photon counting fluorimeter (Horiba - Jobin Yvon) with pulse duration of 1.2 ns (slit width of 2/2, λ_{em} is 473 nm for **1** and 454 nm for **2**). Average fluorescence lifetimes (τ_{av}) for the exponential iterative fitting were calculated from the decay times (τ_i) and the relative amplitudes (a_i) using the following relation

$$\tau_{\text{av}} = (a_1\tau_1^2 + a_2\tau_2^2 + a_3\tau_3^2)/(a_1\tau_1 + a_2\tau_2 + a_3\tau_3)$$

Where a_1 , a_2 and a_3 are the relative amplitudes and τ_1 , τ_2 , and τ_3 are the lifetime values, respectively. For data fitting, a DAS6 analysis software version 6.2 was used.⁴²

Theoretical Calculations. The molecules **1** and **2** were individually first energy-minimized in gas phase using the B3LYP/6-31G* method. By using the minimized structures, HOMO-LUMO levels of each molecule were calculated. Then $\text{p}K_{\text{a}}$ of the compounds **1** and **2** were calculated theoretically using SPARC software (<http://ibmlc2.chem.uga.edu/sparc>, accessed on 11.03.2013).⁴³

RESULTS AND DISCUSSION

The conjugate chromophoric pyridine-end *p*-phenylenevinylene analogue **1** was prepared as reported earlier.^{44,45} Compound **2** having a modified conjugation length was prepared through a carbonyl-nucleophile addition protocol using isoniazid and the corresponding dialdehyde.⁴⁶ The compounds were fully characterized as given in the Supporting Information.

Sensing in Aqueous Medium. The interaction of each compound **1** and **2** toward NACs was first checked in pure water (pH 7). Compound **1** showed rapid fluorescence quenching in presence of both TNP (~ 5 fold) and DNP

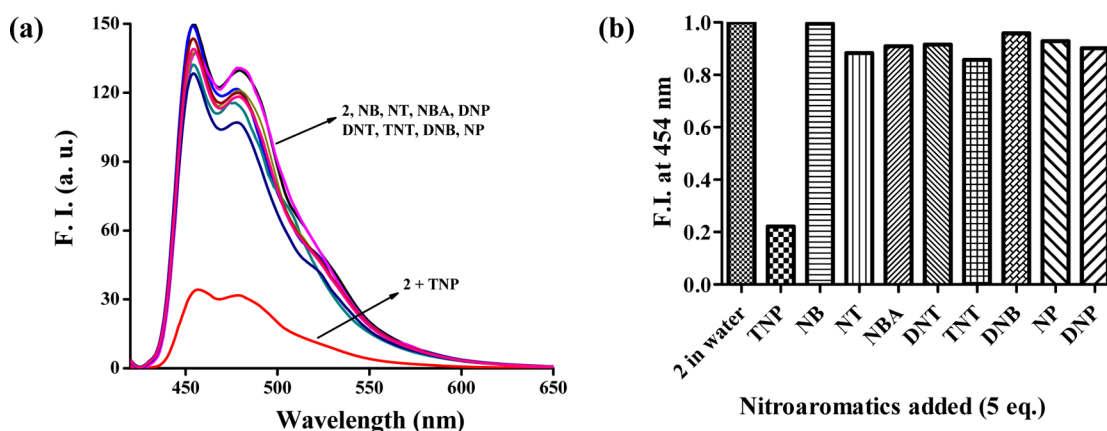


Figure 1. (a) Response of the probe **2** ($10 \mu\text{M}$, λ_{ex} 390 nm) toward different NACs (2 equiv.) in water (pH 7.0). (b) Normalized plots of fluorescence emission at 454 nm of **2** upon addition of different NACs in water (pH 7.0).

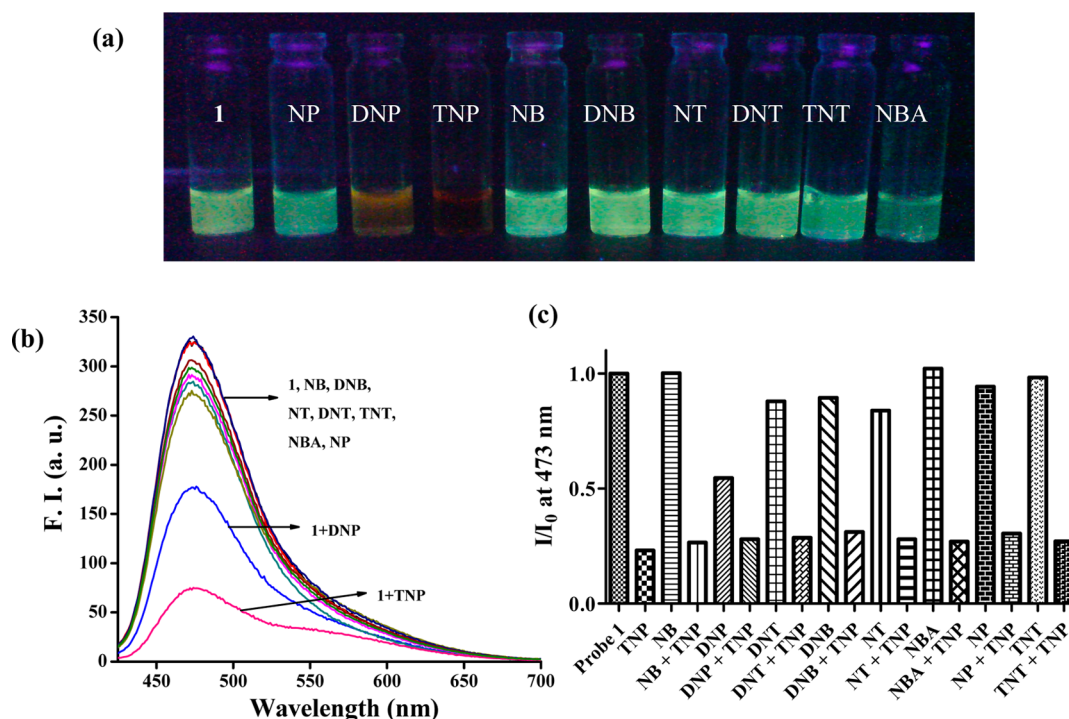


Figure 2. (a) Visual changes in color under a 365 nm UV lamp of **1** ($20 \mu\text{M}$) in presence of different NACs (5 equiv.) in Brij-58 micelles (1 mM). (b) Response of the probe **1** ($10 \mu\text{M}$, λ_{ex} 400 nm) toward different NACs (5 equiv.) in Brij-58 (1 mM) micelles. (c) Interference of different NACs present in excess (12 equiv.) in the detection of TNP (5 equiv.) using **1** in micellar media. [**1**] = $10 \mu\text{M}$ in each case.

(~ 3.4 fold) whereas probe **2**, having an increased H-bonding motif showed selective quenching only with TNP (~ 4.5 fold) (Figure 1 and Figure S1 in the Supporting Information). Though the probes showed a good response in pure water, their aqueous solutions were found to be not very stable and started precipitating after ~ 8 h, possibly because of aggregation. To enhance the solution stability of the probes in water, we therefore incorporated them in different micellar media.

Sensing in Micellar Medium. An aqueous solution of **1** ($10 \mu\text{M}$) was prepared in a neutral micellar Brij-58 medium which was found to be stable for few months. This solution showed absorption spectral peaks at 409, 332, and 275 nm and a strong emission peak at 473 nm ($\lambda_{\text{ex}} = 400$ nm, see Figure S2 in the Supporting Information).

Addition of different NACs into this solution led to notable emission quenching in case of DNP (~ 2 fold) and TNP (~ 4.5

fold), whereas the effect of addition of other NACs were insignificant (Figure 2a, 2b). Titration of **1** showed saturation in the spectral changes with only 5 equiv. of either DNP or TNP (Figure S3, SI). A 1:2 stoichiometry of interaction of **1** with both DNP and TNP was revealed from the Job's plot⁴⁷ and the corresponding binding constants ($\log \beta$) of 9.25 ± 0.02 and 9.36 ± 0.01 , respectively, were obtained using Benesi–Hildebrand method⁴⁸ (see Figure S4 in the Supporting Information). Respective Stern–Volmer quenching constants (K_{sv}) were as high as $2.67 \times 10^4 \text{ M}^{-1}$ and $4.21 \times 10^4 \text{ M}^{-1}$ (see Figure S3 in the Supporting Information) and the detection limits of ~ 35 and ~ 22 nM indicate a strong sensitivity of the probe toward the quenching process.⁴⁹ The selectivity of the probe toward DNP and TNP remains intact even in the presence of excess of other NACs, as they do not show any notable interference (Figure 2c).

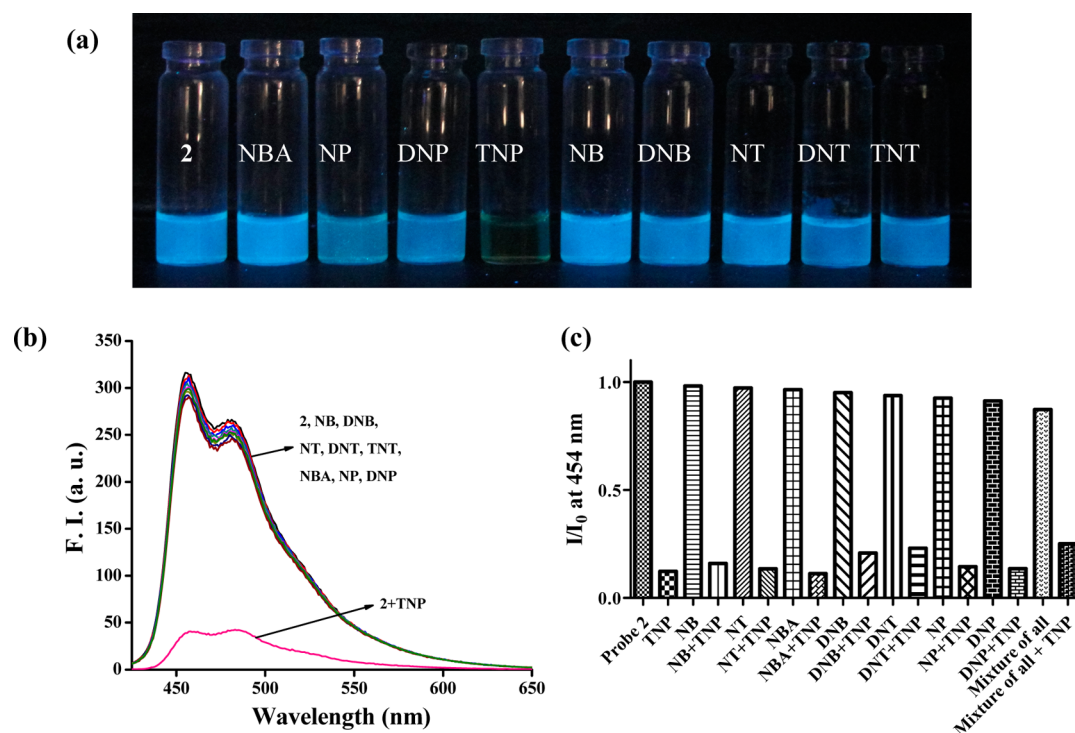


Figure 3. (a) Visual changes in color under a 365 nm UV lamp of **2** (20 μM) in Brij-58 micelles (1 mM) in presence of different NACs (2 equiv.). (b) Response of the probe **2** (10 μM , λ_{ex} 390 nm) toward different NACs (2 equiv.) in Brij-58 (1 mM) micelles. (c) Interference of different NACs present in excess (5 equiv.) in the detection of TNP (2 equiv.) using **2** in micellar media. [**2**] = 10 μM in each case.

Similarly, **2** showed absorption spectral maxima at 333 and 440 nm and emission bands at 456 and 480 nm ($\lambda_{\text{ex}} = 390$ nm) in Brij-58 micellar medium (see Figure S5 in the Supporting Information). Interestingly, **2** showed a selective emission quenching (~ 7.5 fold) with TNP while other NACs did not induce any significant changes (Figure 3a, b). In this case, the saturation in the spectral changes for the titration was obtained upon addition of 2 equiv. of TNP, whereas Job's plot still showed a 1:2 stoichiometry of interactions between **2** and TNP and a binding constant ($\log \beta$) of 9.39 ± 0.02 was obtained (see Figure S6 in the Supporting Information). Compared to **1**, probe **2** showed a larger Stern–Volmer quenching constant ($5.51 \times 10^4 \text{ M}^{-1}$) and a lower detection limit (11.8 nM) with TNP indicating that **2** is a superior probe than **1** for TNP sensing (see Figure S6 in the Supporting Information). The probe **2** was found to be selective toward TNP even in the presence of excess of other nitro aromatics as well as in their mixtures (Figure 3c). The response kinetics of probes **1** and **2** for the detection of TNP showed that in both the cases the interaction was instantaneous (see Figure S7 in the Supporting Information).

Similar interactions with DNP and TNP with either **1** or **2** were also observed in cationic (CTAB) or anionic (SDS) micellar media, but the extent of fluorescence quenching was considerably less probably because of the presence of charge on the micellar surface which affects the optimal approach of NACs toward the probes (see Figure S8 in the Supporting Information).

A rapid change in color from pale to deep yellow was observed under naked-eye upon addition of either DNP or TNP in Brij-58 micellar solution of **1** which was evidenced from the appearance of a broad absorption band in the UV–vis spectra (see Figures S9 and S10 in the Supporting

Information). Compound **2** also showed similar color change, which was, however, selective only to TNP.

Mechanism of Detection. To get an insight into the mechanism of sensing, we performed ^1H NMR titration of **1** and **2** with TNP (Figure 4 and Figure S11 in the Supporting Information). Gradual addition of TNP led to downfield shifts of the protons of both **1** and **2** where the extent of shift ($\Delta\delta$) was greater for the pyridine protons. These observations clearly indicate the involvement of the pyridine nitrogen in the initial protonation through TNP in both the cases. Also, the $\Delta\delta$ was greater in case of **2** (0.44 ppm for 'c' proton) compared to **1** (0.2 ppm for 'c' proton). This may be due to higher extent of protonation in case of **2** compared to **1**.

Selectivity of **1** and **2** toward TNP and/or DNP could be explained by considering their pK_a values. Theoretically calculated protonation pK_a of pyridine Ns (using SPARC program) in **1** (5.8) and **2** (3.7) clearly suggest the possibility of complexation with TNP ($\text{pK}_a = 0.38$) and/or DNP ($\text{pK}_a = 4.11$). This initial protonation caused an electrostatic association between the picrate anions and the protonated pyridine ends. To confirm this, the responses of **2** with TNP were monitored in different buffered conditions (pH 2 and 12). In both the cases, **2** showed lower extent of fluorescence quenching with TNP than at pH 7 probably because of the inability to form an association complex (Figure S5).⁵⁰ This was further confirmed by adding either acid (HCl) or alkali (NaOH) directly into the neutral solution of **2**+TNP which showed a recovery of the fluorescence intensity in either case (see Figure S12 in the Supporting Information). The electrostatic association could further promote electron transfer from the electron-rich fluorophore moiety to electron-deficient NACs. This was supported from the time-resolved emission spectral studies of **1** and **2** in Brij-58 which showed biexponential decay for both with an average lifetime of 1.09

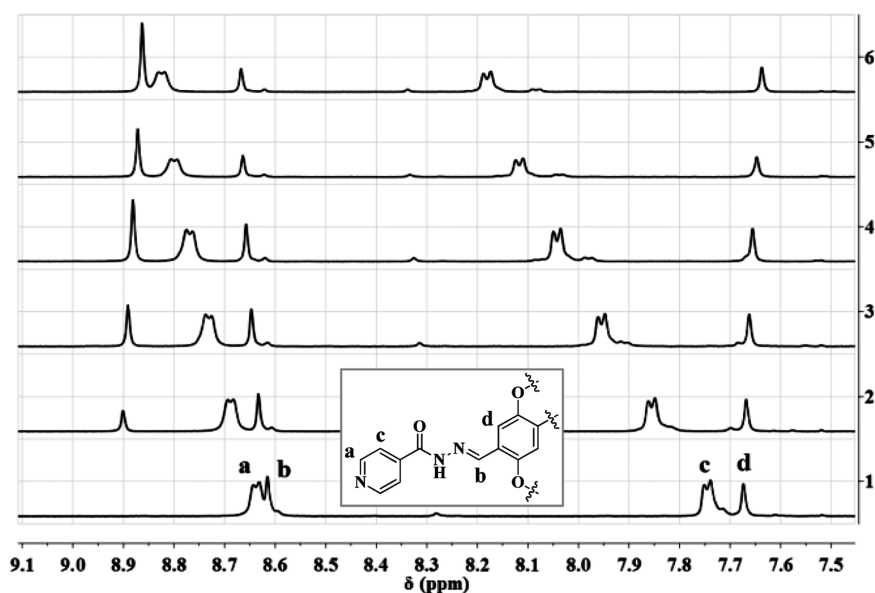


Figure 4. ^1H NMR titration of **2** upon gradual addition of TNP (0, 0.25, 0.5, 0.75, 1.0, 1.5 equiv.) in $\text{CDCl}_3/\text{CD}_3\text{OD}$ (5:1 v/v). Inset showing assigned protons of **2** for convenience.

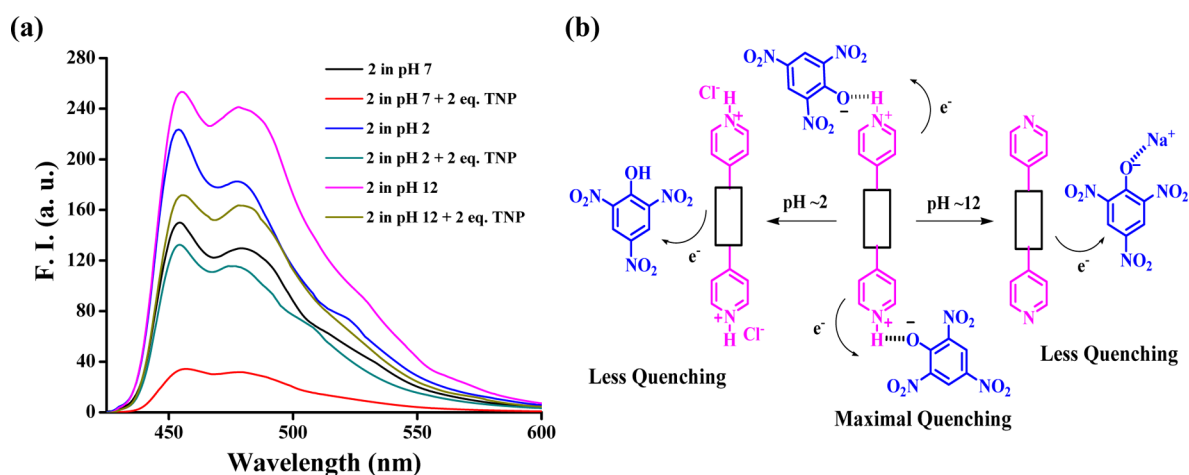


Figure 5. (a) Effect of pH on the interaction of **2** with TNP in water and (b) a scheme of the molecular level interactions involved.

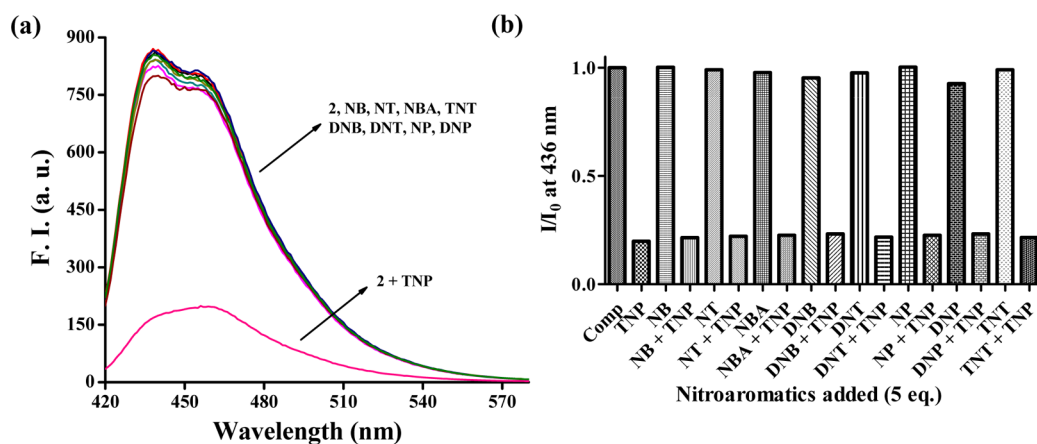


Figure 6. (a) Fluorescence spectra of the probe **2** ($10\ \mu\text{M}$) in THF ($\lambda_{\text{ex}} = 390\ \text{nm}$) with the addition of various nitro aromatics (2 equiv.). (b) Normalized plot of the F. I. at 436 nm for **2** ($10\ \mu\text{M}$) THF with 2 equiv. of TNP in presence of other nitro aromatics in excess. (5 equiv.).

and 0.8 ns, respectively (see Figure S13 in the Supporting Information). Addition of DNP or TNP reduced the average

lifetimes significantly for **1** (0.88 and 0.61 ns for DNP and TNP respectively) and also for **2** (0.55 ns with TNP). The lowering

of average lifetime in both the instances suggests the quenching process as a dynamic phenomenon ($\tau/\tau_0 \neq 1$). The low-lying LUMO of NACs compared to the probes is also a criterion for electron transfer to occur from the probes to NACs. In both the cases, the calculated LUMO energy (using B3LYP/6-31G* theory) of the probes (-2.01 eV for **1** and -2.34 eV for **2**) were found to be higher than that of the corresponding TNP (-3.90 eV).⁵¹ The LUMO energy level of TNP is much lower compared to other nitro aromatics which might be the reason for the facile electron transfer from the protonated probe to TNP.⁵² The high polarizability of picric acid is also an important contributing factor for the higher response toward quenching process over other nitro aromatics.^{53–55}

Sensing in Organic Medium. To enhance the practical utility of the probe as a reusable as well as a portable sensing device we checked their sensing ability in organic solvents. Probe **2** showed a selective emission quenching with TNP (~ 8 fold) in THF medium and the corresponding titrations indicated that only 3 equiv of TNP is required for the saturation of spectral changes (Figure 6a). A larger Stern–Volmer quenching constant ($8.53 \times 10^4 \text{ M}^{-1}$) and a lower detection limit (15.2 nM) obtained for the TNP detection using the probe **2** suggests a significantly strong interaction between them even in organic medium (see Figure S14 in the Supporting Information). The 1:2 stoichiometry of interaction of **2** with TNP was evidenced with a binding constant ($\log \beta$) of 9.61 ± 0.01 (see Figure S14 in the Supporting Information) and the selectivity toward TNP in the presence of excess of other NACs prevailed as with the micellar medium (Figure 6b).

Sensing on Solid Supports. For a rapid on-site detection of TNP we prepared portable test strips by transferring the compound **2** in THF on silica coated aluminum TLC plates (Figure 7a). Onto the plate, the TNP solution (1 ppm) was

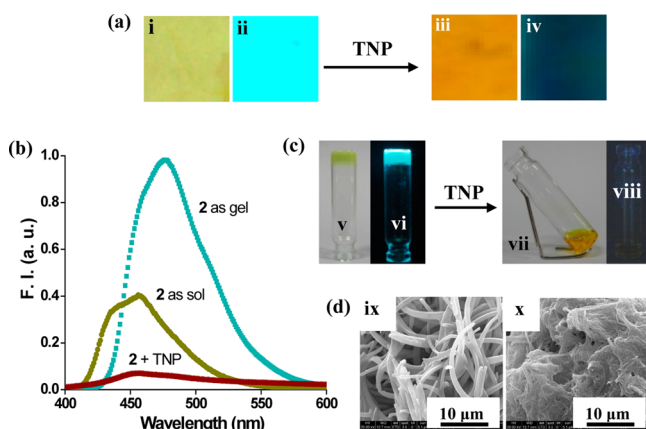


Figure 7. (a) Test strip detection of TNP under (i, iii) day light and (ii, iv) UV light (365 nm); (b) fluorescence spectra of probe **2** in THF (14 mM) in gel and sol state in the absence and presence of 2 equiv. of TNP ($\lambda_{\text{ex}} = 390$ nm); (c) gel of **2** in THF and in presence of TNP under (v, vii) day light and (vi, viii) UV light; (d) SEM image of (ix) **2** and (x) **2**+TNP in THF.

then introduced and immediately the spot could be visualized by vivid color change from yellow to deep orange under the naked eye. The instantaneous quenching of bright blue fluorescence was also noted under a UV-lamp (365 nm).

Sensing in Organogel Matrix. These studies demonstrate that TNP interacts with **2** at the molecular level which prompted us to check the effect of TNP on a supramolecular

assembly. Notably, **2** at higher concentration (14 mM) formed a self-supporting physical gel in THF (Figure 7b,c) via the intermolecular H-bonding through the acylhydrazone groups, π -stacking through the aromatic moieties and van der Waals interactions via their *n*-hexadecyl chains.^{56–59} Thus, a “sol” of **2** at 70 °C showed an emission maximum at 456 nm, whereas upon cooling to room temperature as it formed a gel, it also showed an aggregation-induced enhanced emission⁶⁰ (2.5-fold) with a red-shifted maxima at 477 nm. Interestingly, addition of only 2 equiv of TNP into the gel immediately induced a gel-to-sol transition along with a significant color change from pale yellow to dark yellow (Figure 7b). This indicates that the interaction of **2** with TNP possibly through multiple hydrogen bonding led the breakdown of the gelator assembly and consequent abolition of gels (see Figure S15 in the Supporting Information). Addition of TNP in the gel state led to ~ 14 -fold quenching of the emission intensity with ~ 24 nm blue shift. These observations were further supported from the SEM images, where a complete abolition of the fiber like morphology of **2** occurred only in presence of TNP (Figure 7d and Figure S16 in the Supporting Information). However, this type of abolition of gels could not be induced by other NACs.

CONCLUSION

In conclusion, we have developed for the first time two *p*-phenylenevinylene based probes for the selective detection of both DNP and TNP in pure water as well as in micellar medium. An electron transfer phenomenon from an electron-rich chromophoric probe to the electron deficient NACs appear to operate here. The selectivity in sensing depends on the pK_a of the probes as well as the NACs under consideration. As the water-based sensors may have limitation of use as solid portable device, interaction of TNP with sensor **2** was also studied in THF medium and the portable test strips were made successfully for rapid on-sight detection purpose. Our studies also provide useful insight on the mechanism of interaction of nitro-aromatic explosives with the small molecular probes in aqueous as well as in organic media. This opens up ample scope for developing new molecular probes of better sensitivity across multiple media and also on solid supports.

ASSOCIATED CONTENT

Supporting Information

Synthesis, additional fluorescence spectra, and microscopic (SEM) images described in this paper. This material is available free of charge via the Internet at <http://pubs.acs.org>.

AUTHOR INFORMATION

Corresponding Author

*E-mail: sb@orgchem.iisc.ernet.in. Tel: (+) 080-2293 2664. Fax: (+91) 080-2360-0529.

Notes

The authors declare no competing financial interest.

ACKNOWLEDGMENTS

S.B. thanks DST (J. C. Bose Fellowship) for the financial support of this work. N.D. thanks CSIR for a JRF fellowship.

REFERENCES

- (1) Germain, M. E.; Knapp, M. J. *Chem. Soc. Rev.* **2009**, *38*, 2543–2555.
- (2) <http://www.nolandmines.com/explosivesinmines.htm>.

- (3) Sylvia, J. M.; Janni, J. A.; Klein, J. D.; Spencer, K. M. *Anal. Chem.* **2000**, *72*, 5834–5840.
- (4) Krausa, M.; Schorb, K. *J. Electroanal. Chem.* **1999**, *461*, 10–13.
- (5) Hakansson, K.; Coorey, R. V.; Zubarev, R. A.; Talrose, V. L.; Hakansson, P. *J. Mass Spectrom.* **2000**, *35*, 337–346.
- (6) Jiang, Y.; Zhao, H.; Zhu, N.; Lin, Y.; Yu, P.; Mao, L. *Angew. Chem., Int. Ed.* **2008**, *47*, 8601–8604.
- (7) Ma, Y.; Li, H.; Peng, S.; Wang, L. *Anal. Chem.* **2012**, *84*, 8415–8421.
- (8) Dasary, S. S. R.; Singh, A. K.; Senapati, D.; Yu, H.; Ray, P. C. *J. Am. Chem. Soc.* **2009**, *131*, 13806–13812.
- (9) Feng, L.; Li, H.; Qu, Y.; Lu, C. *Chem. Commun.* **2012**, *48*, 4633–4635.
- (10) Thomas, S. W., III; Joly, G. D.; Swager, T. M. *Chem. Rev.* **2007**, *107*, 1339–1386.
- (11) Kim, D. S.; Lynch, V. M.; Nielsen, K. A.; Johnsen, C.; Jeppesen, J. O.; Sessler, J. L. *Anal. Bioanal. Chem.* **2009**, *395*, 393–400.
- (12) He, G.; Peng, H.; Liu, T.; Yang, M.; Zhang, Y.; Fang, Y. *J. Mater. Chem.* **2009**, *19*, 7347–7353.
- (13) Hu, Y. J.; Tan, S. Z.; Shen, G. L.; Yu, R. Q. *Anal. Chim. Acta* **2006**, *570*, 170–175.
- (14) Nie, H.; Zhao, Y.; Zhang, M.; Ma, Y.; Baumgarten, M.; Mullen, K. *Chem. Commun.* **2011**, *47*, 1234–1236.
- (15) Nagarkar, S. S.; Joarder, B.; Chaudhari, A. K.; Mukherjee, S.; Ghosh, S. K. *Angew. Chem., Int. Ed.* **2013**, *52*, 2881–2885.
- (16) Costa, A. I.; Prata, V. *Sens. Actuators B Chem.* **2012**, *161*, 251–260.
- (17) Tao, S.; Li, G.; Zhu, H. *J. Mater. Chem.* **2006**, *16*, 4521–4528.
- (18) Alizadeha, T.; Zareb, M.; Ganjalib, M. R.; Norouzib, P.; Tavanab, B. *Biosens. Bioelectron.* **2010**, *25*, 1166–1172.
- (19) Lee, Y. H.; Liu, H.; Lee, J. Y.; Kim, S. H.; Kim, S. K.; Sessler, J. L.; Kim, Y.; Kim, J. S. *Chem.—Eur. J.* **2010**, *16*, 5895–5901.
- (20) Zhang, C.; Che, Y.; Yang, X.; Bunes, B. R.; Zang, L. *Chem. Commun.* **2010**, *46*, 5560–5562.
- (21) Naddo, T.; Che, Y.; Zhang, W.; Balakrishnan, K.; Yang, X.; Yen, M.; Zhao, J.; Moore, J. S.; Zang, L. *J. Am. Chem. Soc.* **2007**, *129*, 6978–6979.
- (22) Yang, Y.; Wang, H.; Su, K.; Long, Y.; Peng, Z.; Li, N.; Liu, F. *J. Mater. Chem.* **2011**, *21*, 11895–11900.
- (23) Salinas, Y.; Manez, R. M.; Marcos, M. D.; Sancenon, F.; Costero, A.; Parra, M.; Gil, S. *Chem. Soc. Rev.* **2012**, *41*, 1261–1296.
- (24) Rana, A.; Panda, P. K. *RSC Adv.* **2012**, *2*, 12164–12168.
- (25) Zyryanov, G. V.; Palacios, M. A.; Anzenbacher, P. *Org. Lett.* **2008**, *10*, 3681–3684.
- (26) Kumar, M.; Vij, V.; Bhalla, V. *Langmuir* **2012**, *28*, 12417–12421.
- (27) Pandya, A.; Goswami, H.; Lodhab, A.; Menon, S. K. *Analyst* **2012**, *137*, 1771–1774.
- (28) Harris, A. H.; Binkley, O. F.; Chenoweth, B. M. *Am. J. Public Health* **1946**, *36*, 727–733.
- (29) Shen, J.; Zhang, J.; Zuo, Y.; Wang, L.; Sun, X.; Li, J.; Han, W.; He, R. *J. Hazard. Mater.* **2009**, *163*, 1199–1206.
- (30) Wyman, J. F.; Serve, M. P.; Hobson, D. W.; Lee, L. H.; Uddin, D. E. *J. Toxicol. Environ. Health, Part A* **1992**, *37*, 313–327.
- (31) Anderson, G.; Lamar, J. D.; Charles, P. T. *Environ. Sci. Technol.* **2007**, *41*, 2888–2893.
- (32) Peng, Y.; Zhang, A. J.; Dong, M.; Wang, Y. W. *Chem. Commun.* **2011**, *47*, 4505–4507.
- (33) Bhalla, V.; Gupta, A.; Kumar, M. *Org. Lett.* **2012**, *14*, 3112–3115.
- (34) Xu, Y.; Li, B.; Li, W.; Zhao, J.; Sun, S.; Pang, Y. *Chem. Commun.* **2013**, *49*, 4764–4766.
- (35) Venkatramiah, N.; Kumar, S.; Patil, S. *Chem. Commun.* **2012**, *48*, 5007–5009.
- (36) An, Z. F.; Zheng, C.; Chen, R. F.; Yin, J.; Xiao, J. J.; Shi, H. F.; Tao, Y.; Qian, Y.; Huang, W. *Chem.—Eur. J.* **2012**, *18*, 15655–15661.
- (37) Bhalla, V.; Pramanik, S.; Kumar, M. *Chem. Commun.* **2013**, *49*, 895–897.
- (38) Roy, B.; Bar, A. K.; Gole, B.; Mukherjee, P. S. *J. Org. Chem.* **2013**, *78*, 1306–1310.
- (39) Kumari, N.; Dey, N.; Jha, S.; Bhattacharya, S. *ACS Appl. Mater. Interfaces* **2013**, *5*, 2438–2445.
- (40) Singh, Y.; Gulyani, A.; Bhattacharya, S. *FEBS Lett.* **2003**, *541*, 132–136.
- (41) Bhattacharya, S.; Gulyani, A. *Chem. Commun.* **2003**, 1158–1159.
- (42) Lakowicz, J. R., in *Principles of Fluorescence Spectroscopy*, 3rd ed.; Springer: New York, 2006; pp 192.
- (43) Herrero-Martinez, J. M.; Sanmartin, M.; Roses, M.; Bosch, E.; Rafols, C. *Electrophoresis* **2005**, *26*, 1886–1895.
- (44) Samanta, S. K.; Bhattacharya, S. *Chem. Commun.* **2013**, *49*, 1425–1427.
- (45) Samanta, S. K.; Pal, A.; Bhattacharya, S. *Langmuir* **2009**, *25*, 8567–8578.
- (46) Wang, B.; Wasielewski, M. R. *J. Am. Chem. Soc.* **1997**, *119*, 12–21.
- (47) Job, P. *Ann. Chim.* **1928**, *9*, 113–203.
- (48) Hildebrand, B. H. *J. Am. Chem. Soc.* **1949**, *71*, 2703–2707.
- (49) Ballesteros, E.; Moreno, D.; Gomez, T.; Rodriguez, T.; Rojo, J.; Valverde, M. G.; Torroba, T. *Org. Lett.* **2009**, *11*, 1269–1272.
- (50) Liu, T.; Ding, L.; He, G.; Yang, Y.; Wang, W.; Fang, Y. *ACS Appl. Mater. Interfaces* **2011**, *3*, 1245–1253.
- (51) Sanchez, J. C.; DiPasquale, A. G.; Rheingold, A. L.; Trogler, W. C. *Chem. Mater.* **2007**, *19*, 6459–6470.
- (52) Yang, J.-S.; Swager, T. M. *J. Am. Chem. Soc.* **1998**, *120*, 11864–11873.
- (53) Sohn, H.; Sailor, M. J.; Magde, D.; Trogler, W. C. *J. Am. Chem. Soc.* **2003**, *125*, 3821–3830.
- (54) Thomas, S. W., III; Amara, J. P.; Bjork, R. E.; Swager, T. M. *Chem. Commun.* **2005**, 4572–4574.
- (55) Bhalla, V.; Gupta, A.; Kumar, M.; Shankar Rao, D. S.; Krishna Prasad, S. *ACS Appl. Mater. Interfaces* **2013**, *5*, 672–679.
- (56) Kartha, K. K.; Babu, S. S.; Srinivasan, S.; Ajayaghosh, A. *J. Am. Chem. Soc.* **2012**, *134*, 4834–4841.
- (57) Samanta, S. K.; Bhattacharya, S. *J. Mater. Chem.* **2012**, *22*, 25277–25287.
- (58) Samanta, S. K.; Bhattacharya, S. *Langmuir* **2009**, *25*, 8378–8381.
- (59) Samanta, S. K.; Pal, A.; Bhattacharya, S.; Rao, C. N. R. *J. Mater. Chem.* **2010**, *20*, 6881–6890.
- (60) Li, D.; Liu, J.; Kwok, R. T. K.; Liang, Z.; Tang, B. Z.; Yu, J. *Chem. Commun.* **2012**, *48*, 7167–7169.